
Universiteit
Leiden
The Netherlands

Glcp constitutes the major glucose uptake system of Streptomyces coelicor A A3(2)

Wezel, G.P. van; Mahr, K.; König, M.; Traag, B.A.; Pimentel-Schmitt, E.F.; Willimek, A.; Titgemeyer, F.

Citation
Wezel, G. P. van, Mahr, K., König, M., Traag, B. A., Pimentel-Schmitt, E. F., Willimek, A., & Titgemeyer, F. (2005). Glcp constitutes the major glucose uptake system of Streptomyces coelicor A A3(2). *Molecular Microbiology*, *55*(2), 624-636. doi:10.1111/j.1365-2958.2004.04413.x

Version:	Publisher's Version
License:	Licensed under Article 25fa Copyright Act/Law (Amendment Taverne)
Downloaded from:	https://hdl.handle.net/1887/3203733

Note: To cite this publication please use the final published version (if applicable).

Molecular Microbiology (2005) **55**(2), 624–636 doi:10.1111/j.1365-2958.2004.04413.x

GlcP constitutes the major glucose uptake system of *Streptomyces coelicolor* A3(2)

Gilles P. van Wezel,[2†] Kerstin Mahr,[1†] Miriam König,[1†] Bjørn A. Traag,[2] Elisângela F. Pimentel-Schmitt,[1] Andreas Willimek[1] and Fritz Titgemeyer[1]*

[1]*Lehrstuhl für Mikrobiologie, Friedrich-Alexander-Universität Erlangen-Nürnberg, 91058 Erlangen, Germany.*

[2]*Department of Biochemistry, LIC, Leiden University, PO BOX 9502, 2300 RA Leiden, the Netherlands*

Summary

We provide a functional and regulatory analysis of *glcP*, encoding the major glucose transporter of *Streptomyces coelicolor* A3(2). GlcP, a member of the Major Facilitator Superfamily (MFS) of bacterial and eucaryotic sugar permeases, was found to be encoded twice at two distinct loci, *glcP1* and *glcP2*, located in the central core and in the variable right arm of the chromosome respectively. Heterologous expression of GlcP in *Escherichia coli* led to the full restoration of glucose fermentation to mutants lacking glucose transport activity. Biochemical analysis revealed an affinity constant in the low-micromolar range and substrate specificity for glucose and 2-deoxyglucose. Deletion of *glcP1* but not *glcP2* led to a drastic reduction in growth on glucose reflected by the loss of glucose uptake. This correlated with transcriptional analyses, which showed that *glcP1* transcription was strongly inducible by glucose, while *glcP2* transcripts were barely detectable. In conclusion, GlcP, which is the first glucose permease from high G+C Gram-positive bacteria characterized at the molecular level, represents the major glucose uptake system in *S. coelicolor* A3(2) that is indispensable for the high growth rate on glucose. It is anticipated that the activity of GlcP is linked to other glucose-mediated phenomena such as carbon catabolite repression, morphogenesis and antibiotic production.

Introduction

Streptomycetes are Gram-positive soil bacteria that are widely used as producers of antibiotics and many other beneficial compounds (Bibb, 1996; Baltz, 1998). In nature, they contribute as soil-dwelling bacteria substantially to the degradation of dead plant and animal material by their ability to utilize a wide variety of complex polysaccharides, including cellulose, xylan and chitin (Hodgson, 2000). This is achieved by the action of exoenzymes that break down the polysaccharides to mono- and disaccharides, which are internalized by specific carbohydrate uptake systems. More than 50 carbohydrate permeases were identified on the *Streptomyces coelicolor* A3(2) genome (Bertram *et al*., 2004). A few have been described at the molecular level in various streptomycetes. Cellobiose/cellotriose, maltose, trehalose and xylobiose are taken up via ATP-driven ABC transport systems, while fructose and *N*-acetylglucosamine are transported by the phosphotransferase system (PTS) (Hurtubise *et al*., 1995; Schlösser and Schrempf, 1996; Schlösser *et al*., 1997; Schlösser, 2000; Wang *et al*., 2002; Nothaft *et al*., 2003a,b).

The molecular nature of the glucose uptake system of streptomycetes, which is considered the most favourable nutrient in these organisms, is unknown. This lack of information is surprising as many glucose-mediated processes, including antibiotic production, morphogenesis and carbon catabolite repression (CCR), are under intensive investigation (Pope *et al*., 1996; van Wezel *et al*., 1997; Escalante *et al*., 1999; Ueda *et al*., 2000; Kim *et al*., 2001; Seo *et al*., 2002). A number of glucose-negative strains have been isolated as mutants resistant to the toxic analogon 2-deoxyglucose (Hodgson, 1982; Kwakman and Postma, 1994). As the mutations all map to the gene encoding glucose kinase and none to a transporter-encoding gene, it became obvious that more than one glucose permease must exist. The presence of a constitutive, low-affinity transport system has been reported for *S. coelicolor* and *Streptomyces violaceoruber* with affinity constants of 6.1 mM and 1 mM (Sabater and Asensio, 1973; Hodgson, 1982). In the course of a study on ABC-type disaccharide transporters, it was noted that *Streptomyces lividans* has a high- and low-affinity glucose uptake activity with affinity constants of 120 μM and 6.2 mM (Hurtubise *et al*., 1995). The isolation of a glucose-utilization mutant from the naturally glucose-negative *Streptomyces clavuligerus* wild-type strain revealed a glucose permease with a broader substrate specificity that is energized by the proton motive force (Garcia-Dominguez *et al*., 1989).

Accepted 27 September, 2004. *For correspondence. E-mail ftitgem@biologie.uni-erlangen.de; Tel. (+49) 9131 852 8084; Fax (+49) 9131 852 8082. †These authors contributed equally to this work.

© 2004 Blackwell Publishing Ltd

None of these permeases have been characterized at the molecular level.

In search for a possible glucose permease, we previously detected GlcP in the genome of *S. coelicolor* A3(2), a permease of the major facilitator superfamily (MFS) that shares 51% protein identity to a glucose permease of *Synechocystis* (Zhang *et al*., 1989; Bertram *et al*., 2004). Interestingly, GlcP is encoded twice on the chromosome by the genes *glcP1* (SCO5578) and *glcP2* (SCO7153), which differ only in one base pair giving rise to a silent mutation and thus produce identical gene products. In this communication, we provide a biochemical analysis of GlcP. We further describe its *in vivo* role and transcriptional regulation through mutational dissection of *glcP1* and *glcP2*, which shows that GlcP is the major glucose transporter in *S. coelicolor* A3(2) that is indispensable for maintaining a high growth rate on glucose.

Results

To characterize glucose internalization in *S. coelicolor* A3(2), we determined the kinetic parameters and the inducibility of glucose uptake. Glucose transport assays were conducted with strain M145 grown in mineral medium supplemented with glycerol or glycerol plus glucose. As depicted in Fig. 1A, uptake of glucose was strongly induced in the presence of glucose. Measurement of the initial uptake rates at various glucose concentrations revealed an overall glucose uptake activity into mycelia with an apparent K_m of 137 ± 16.5 μM and with a V_{max} of 22 ± 2.4 nmol per minute per mg dry weight (Fig. 1B).

Functionality of GlcP resolved by heterologous expression

In the course of an *in silico* screen for carbohydrate uptake systems present in the genome of *S. coelicolor* A3(2), we have recently predicted that GlcP may function as a glucose permease (Bertram *et al*., 2004). GlcP is a member of the MFS, which comprises H^+/symporters and facilitator proteins (Pao *et al*., 1998; Bertram *et al*., 2004). GlcP is encoded by two duplicated genes, where one is situated in the constant region of the chromosome (SCO5578, *glcP1*) and one is found in the variable right arm of the chromosome (SCO7153, *glcP2*) (Fig. 2). Both genes encode identical gene products of 472 amino acids. The duplicated area includes 36 bp of upstream region containing a 16 nt palindrome sequence that could serve as a transcription factor binding site (Fig. 2). The homology ends exactly with the stop codon, and the genes are followed by non-related stem loop structures forming potential transcriptional termination signals. The deduced sequence exhibits 51%, 32% and around 30% overall identity to the glucose transporters GlcP of *Synechocystis* PCC6803 and Glf of *Zymomonas mobilis*, and to mammalian glucose permeases, respectively, and between 28% and 37% amino acid identity to bacterial uptake systems specific for arabinose, galactose or xylose (Zhang *et al*., 1989; Weisser *et al*., 1995; Pao *et al*., 1998).

To examine the function of GlcP, we expressed the gene in *Escherichia coli*. The *glcP*-coding region was cloned by polymerase chain reaction (PCR) from the *S. coelicolor* A3(2) M145 genome, and inserted into vector pSU2718 behind the *lacZ* promoter, yielding pFT76. The glucose-negative *E. coli* strains LR2-175 and LM1 that lack detectable glucose transport activity were transformed with pFT76. The transformants were streaked onto MacConkey agar plates supplemented with 50 mM glucose (Fig. 3A). LR2-175(pFT76) and LM1(pFT76) formed red colonies because of the fermentation of glucose, while non-glucose-fermenting white colonies were observed when the strains carried the control plasmid pSU2718. Subsequent glucose uptake measurements showed that glucose was efficiently internalized in *E. coli* strain LR2-175(pFT76), while no transport was observed for transformants harbouring the control plasmid without *glcP* (Fig. 3B). Hence, heterologous expression of *glcP* in *E. coli* identified GlcP as a glucose permease.

The function of *S. coelicolor* GlcP was studied in more detail. Therefore, we took advantage of heterologously produced GlcP in *E. coli* LR2-175(pFT76), which

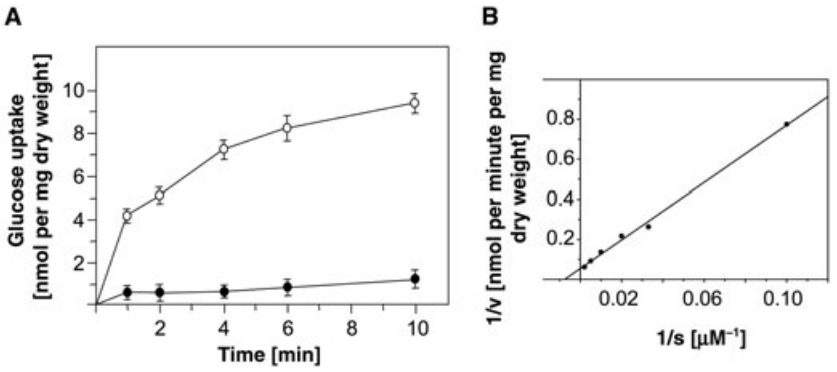

Fig. 1. Glucose transport in *S. coelicolor* A3(2).
A. Glucose uptake as a function of time. Mycelia of *S. coelicolor* A3(2) M145 were grown in mineral medium containing 0.1% casamino acids and supplemented with either 50 mM glycerol (non-inducing growth conditions; ●) or 50 mM glycerol plus 50 mM glucose (inducing growth conditions; ○). Standard deviations of triplicate data points are shown by error bars.
B. Lineweaver–Burk plot of glucose uptake rates of *S. coelicolor* A3(2) M145 as a function of glucose concentration. K_m and V_{max} were calculated from three experiments.

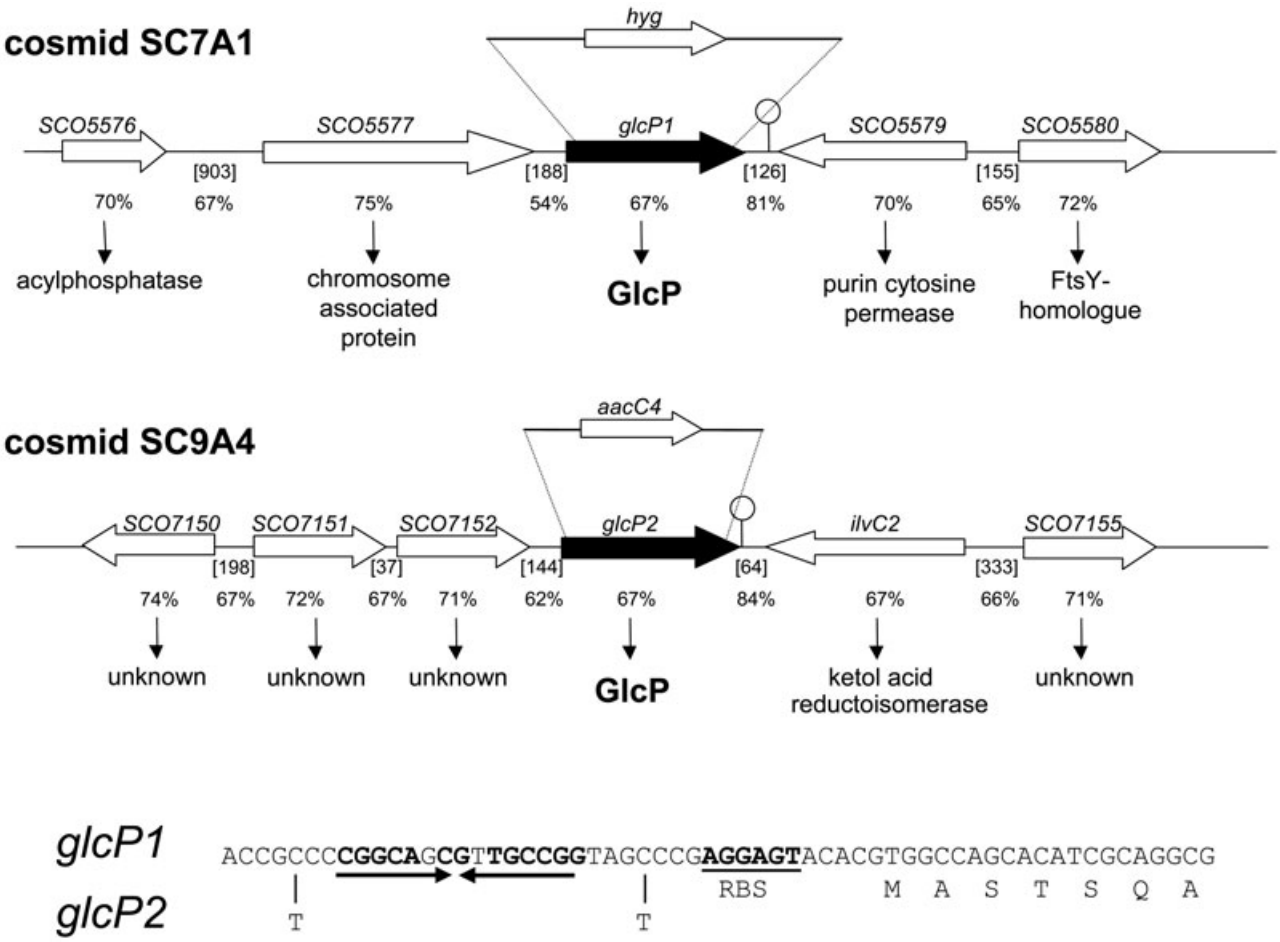

Fig. 2. Genetic map of the *glcP1* and *glcP2* loci. Unknown genes are designated with the respective SCO number above and the names of predicted proteins below the genes. The lengths of the intergenic regions are indicated in brackets (in nt). The G+C content of coding and intergenic regions is expressed in percentages. Two putative transcription termination sites are marked as stem loops (CCGCCGCCCCGCCCG GTCGCATTCCGGGCGGGGCGGCGG, 62 nt downstream of *glcP1*; GCAGGCCGGTGGGCGCGCCGCCGTGGCGCGCCCACCGGCCTGC 14 nt downstream of *glcP2*). The relative extensions of *glcP* deletions and the inserted antibiotic resistance gene cassettes are given. The conserved upstream regions of 36 nt including a 16 nt palindromic sequence is shown at the bottom.

was free of any background activity. We measured a K_m of 41 ± 5 μM and a V_{max} of 23 ± 1 nmol min^{-1} OD$_{600}^{-1}$, which means that GlcP is a high-affinity transport system (Fig. 3C). The presence of the ionophores carbonyl cyanid-*m*-chlorophenyl-hydrazone (CCCP) and dinitrophenol (DNP) that both destroy the membrane potential resulted in residual glucose transport activity of 5% and 7%, respectively, whereas the ATP-formation inhibitor *N,N′*dicyclohexylcarbodiimide (DCCD) had no significant influence (Fig. 3D). Concerning the substrate specificity, it was reported that the homologues from *Synechocystis* and *Z. mobilis* transport fructose (Zhang *et al*., 1989; Parker *et al*., 1995; Weisser *et al*., 1995). However, strain LR2-175(pFT76), which lacks a functional fructose permease, exhibited no detectable fructose uptake (data not shown). Subsequent uptake competition experiments confirmed this and showed further that 2-deoxyglucose was readily recognized by GlcP, while this was not the case for methyl α-D-glucopyranoside (Fig. 3E).

Mutational analysis of glcP1 *and* glcP2

After identification of GlcP as a glucose-specific permease, we analysed its role in glucose transport in *S. coelicolor* A3(2). Two single and a double mutant were constructed that carried a deletion in *glcP1* (BAP17), *glcP2* (BAP18), or in both genes (BAP19) respectively. All mutants sporulated normally on mineral and complex media, as judged by phase contrast microscopy. As the genes located downstream of *glcP1* and *glcP2* are oriented in the opposite orientation (Fig. 2), polar effects resulting from the insertion of a resistance cassette in *glcP1* or *glcP2* were highly unlikely.

To assess the ability of the mutants to utilize glucose as sole carbon source, we compared the growth curves

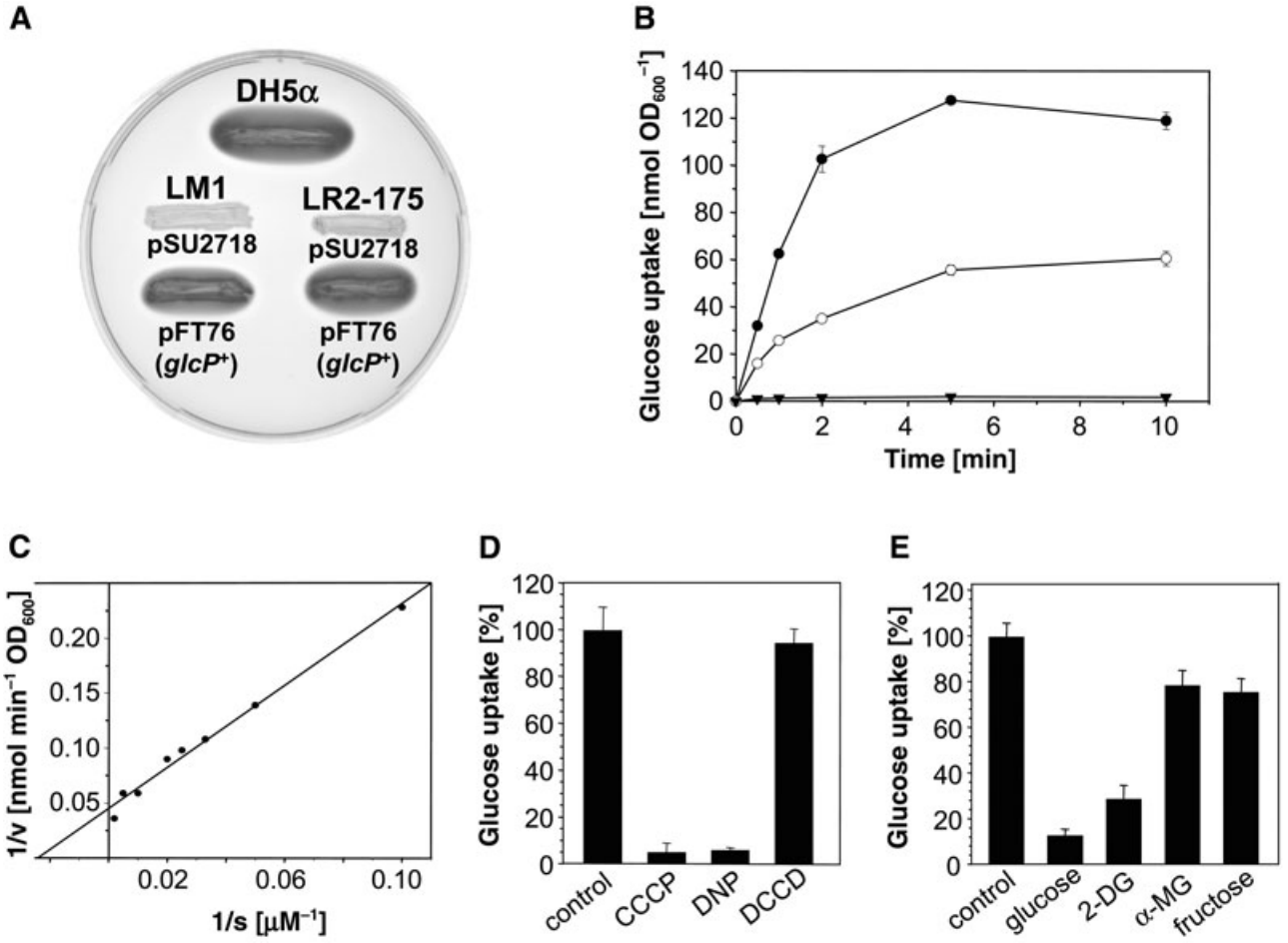

Fig. 3. Identification of the glucose transporter GlcP of *S. coelicolor* A3(2).
A. Complementation of the glucose-negative phenotype in *E. coli*. DH5α(pSU2718) (positive control), LM1(pSU2718) (negative control), LM1(pFT76 *glcP2*$^+$), LR2-175(pSU2718) (negative control) and LR2-175(pFT76 *glcP2*$^+$) were streaked on a MacConkey agar base plate supplemented with 50 mM glucose. Pigmented red colonies (dark grey) indicate the fermentation of glucose, whereas white colonies (light grey) reflect a deficiency in glucose fermentation.
B. Time-dependent uptake of [^{14}C]-glucose of *E. coli* DH5α(pSU2718) (●; positive control), LR2-175(pSU2718) (▼; negative control) and LR2-175(pFT76 *glcP*$^+$) (○).
C. Lineweaver-Burk plot of glucose uptake rates of LR2-175(pFT76) as a function of glucose concentration. K_m and V_{max} were determined from three experiments.
D. Transport inhibition assay using ionophores CCCP (50 μM) and DNP (1 mM), and the ATP-formation inhibitor DCCD (0.5 mM). Transport activity without effectors was set to 100% (control).
E. Glucose uptake competition assay using a 100-fold excess of non-radioactive sugars (10 mM). Transport activity without additional sugar was set to 100% (control).
Standard deviations of triplicate data points are shown by error bars. Very similar results were obtained from three independent experiments. 2DG, 2-deoxyglucose; αMG, methyl α-D-glucopyranoside.

with the parental strain M145. For this purpose, 500 ml NMMP cultures with glucose were inoculated with precultures of the respective strains at an OD_{550} of 0.1 and allowed to grow at 30°C (Fig. 4A). While deletion of *glcP2* in BAP18 did not affect growth on glucose, the *glcP1* mutant BAP17 and the double mutant BAP19 showed clearly reduced growth rates. Monitoring of glucose in the medium showed that the parental M145 and BAP18 immediately utilized glucose. NMMP cultures contained 0.2% casamino acids in addition to glucose, which is sufficient to support initial growth up to OD_{550} of 0.3 (van Wezel *et al*., 1997). Glucose consumption in the two strains lacking *glcP1* started significantly later, corresponding to a time point where the casamino acids became limited (approximately after 10–12 h). A similar experiment with mannitol as the sole carbon source revealed no noticeable difference in growth rates and biomass formation between M145 and the three mutants, showing that the differences indeed resulted from their inability to grow properly on glucose, and not by any other defect (data not shown).

The growth analysis corresponded with the ability of the

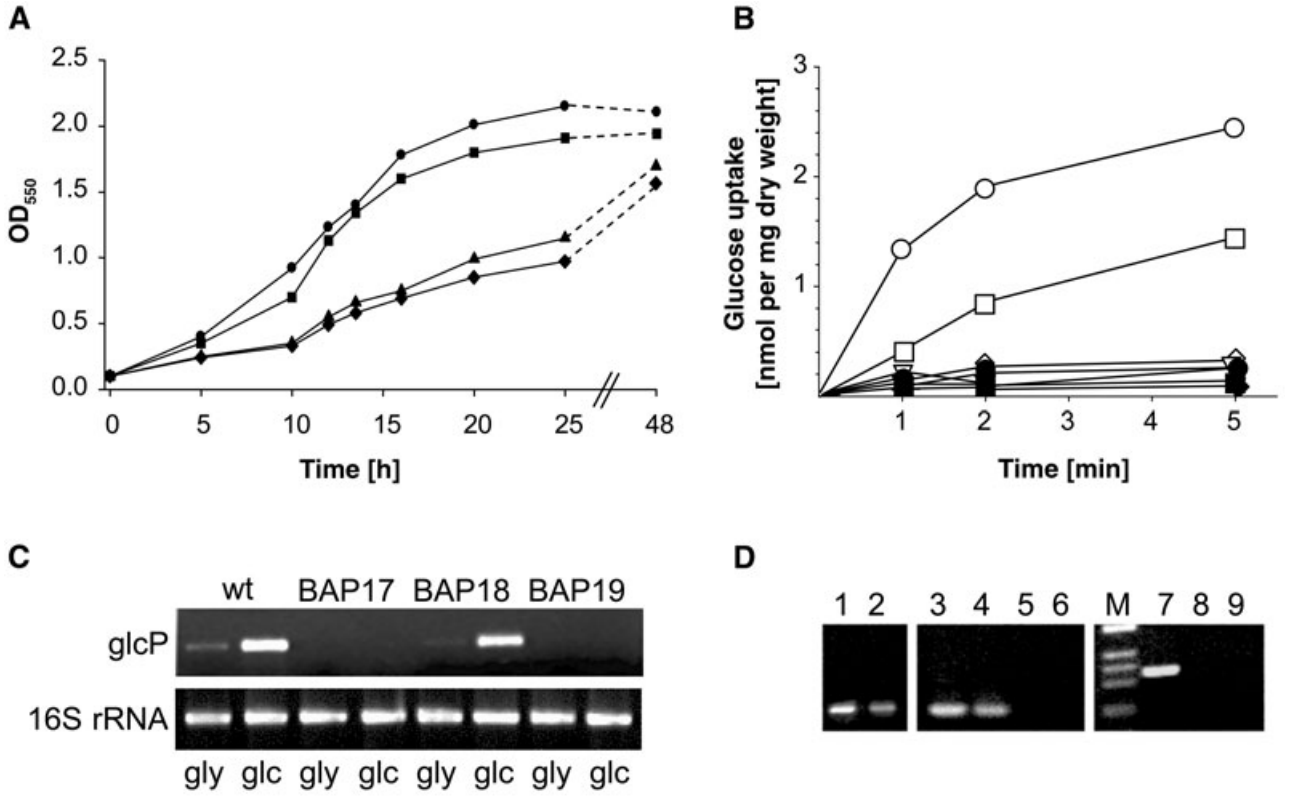

Fig. 4. Growth and expression of *glcP1* and *glcP2*.
A. Growth of *S. coelicolor* A3(2) M145 (●) and *glcP* mutants BAP17 (Δ*glcP1*; ▲), BAP18 (Δ*glcP2*; ■) and BAP19 (Δ*glcP1*Δ*glcP2*; ◆) on NMMP plus 50 mM glucose.
B. Time-course of glucose uptake. Mycelia of *S. coelicolor* A3(2) M145 (●), BAP17 (▲), BAP18 (■) and BAP19 (◆) were grown in mineral medium containing 0.1% casamino acids and 50 mM glycerol (closed symbols) or 50 mM glycerol plus 50 mM glucose (open symbols). Data were reproduced by three experiments.
C. RT-PCR of *glcP* transcripts of *S. coelicolor* A3(2) M145 and *glcP* mutants. A 1% agarose gel shows RT-PCR amplification products of *glcP1/2*-mRNA after cycle 24. Total RNA was prepared from cultures grown on mineral medium supplemented with 0.1% casamino acids and 50 mM glycerol in the presence (glc) and absence of 50 mM glucose (gly).
D. Identification of *glcP2* and anti-sense transcripts by RT-PCR. Left: identification of *glcP2* transcripts in RNA from *S. coelicolor* A3(2) M145, using extended RT-PCR (35 cycles) and allele-specific primers. Lane 1: saturated signal of *glcP1* (primers GlcP1-RTF + GlcP-RTR); lane 2: weaker signal for *glcP2* (primers GlcP2-RTF + GlcP-RTR). Middle: RT-PCR using 25 cycles shows *glcP1* transcripts present in RNA from *S. coelicolor* A3(2) M145 (lane 3) and from *glcP2* mutant BAP18 (lane 4). Lanes 5 and 6 present controls of lanes 3 and 4, respectively, showing the absence of RT-PCR product when the cDNA synthesis (RT) step was omitted. Note that *glcP1* transcripts are less abundant in the *glcP2* mutant (probably because of the anti-sense transcript visualized in lane 7). Right: identification of anti-sense transcripts in the *glcP2* mutant. Lane 7: anti-sense RNA product generated by RT-PCR from RNA from BAP18 (primers apra-up + GlcP2-RTF); lane 8: same as lane 7, but without RT step (control to confirm the absence of genomic DNA); lane 9: same as lane 7, but with RNA isolated from M145 instead of the *glcP2* mutant. To ascertain that only anti-sense transcripts could be identified, the cDNA synthesis step was carried out in the presence of only the *glcP2*-specific (forward) primer. M: DNA size marker (from top to bottom: 517, 396, 344, 298, and double band of 220/201 bp).

mutants to incorporate glucose, which was substantial in the presence of an intact *glcP1* gene and barely detectable in strains carrying a *glcP1* deletion (Fig. 4B). Expectedly, glucose transport was negligibly low in the *glcP1* mutant. Thus, we conclude that *glcP1* alone accounts for maintenance of the high growth rate on glucose, which is in agreement with the growth analysis presented above. Surprisingly, glucose transport in the *glcP2* mutant was only about 50–60% of the wild-type level, suggesting that perhaps *glcP1* is expressed at a lower level in the Δ*glcP2* background as compared with the parental M145. This was confirmed by our reverse transcription polymerase chain reaction (RT-PCR) data, and most probably results from the production of an anti-sense transcript from the apramycin resistance cassette inside the *glcP*2 gene (see below).

Transcription analysis by RT-PCR

Total *glcP* (*glcP1* + *glcP2*) transcript levels in M145 and its *glcP* mutant derivatives were quantitatively determined by semi-real-time RT-PCR, using primers GlcP-RT1 and GlcP-RT2 that hybridized perfectly to both genes. As can be inferred from Fig. 4C, *glcP* transcripts were readily

detectable in glucose-grown M145 (total *glcP*-mRNA) and in the *glcP2* mutant BAP18 (allowing the detection of only *glcP1*-mRNA), while only marginal *glcP* expression was observed in glycerol-grown cultures. Under these conditions, we failed to detect transcripts in the *glcP1* mutant, or – expectedly – in the double mutant BAP19.

Similar experiments were also carried out using gene-specific primers, to allow discrimination between *glcP1*- and *glcP2*-derived mRNA. Therefore, we used oligonucleotides GlcP1-RTF and GlcP2-RTF as forward primers, which hybridized specifically to the region around nt position –60 relative to the start of *glcP1* or *glcP2* respectively. The reverse primer (GlcP-RTR) was chosen around nt position +130, so as to recognize both genes. Considering the expected difference in mRNA levels of *glcP1*- and *glcP2*-derived transcripts, we performed semi-real-time PCR, analysing samples at three-cycle intervals. After the maximal 35 amplification cycles, a very strong and saturated signal was observed for *glcP1*, and a weak band for *glcP2* (Fig. 4D, lanes 1 and 2). The intensity of the *glcP2*-derived band obtained after 35 cycles corresponded to the band obtained from *glcP1*-derived transcripts after only 21 cycles (data not shown), illustrating the large difference in expression level (see also below). A control experiment without reverse transcriptase did not show any PCR product (lanes 5 and 6), showing that the bands were transcript specific.

Interestingly, *glcP1*-derived transcripts were significantly lower in the *glcP2* mutant as compared with M145 (Fig. 4C and D). We anticipated the possibility that an anti-sense transcript would be produced in the *glcP2* mutant, which would hybridize perfectly over a stretch of 64 nt to nt positions –36/+28 of the *glcP1*-mRNA, and would therefore interfere with *glcP1* expression (see also Fig. 2). To test this, we performed an RT-PCR experiment using primers GlcP2-RTF and apra-up, which were specific for the *glcP2* upstream region and the start of the apramycin resistance cassette respectively. cDNA was produced in the presence of only GlcP2-RTF, reverse transcriptase was inactivated, after which primer apra-up was added and the PCR amplification was performed. In this way, only anti-sense transcripts could be amplified. As can be derived from Fig. 4D (lane 7), a clear and strong band was produced, showing that indeed significant amounts of anti-sense transcripts were present in the *glcP2* mutant. Control experiments using the same RNA without reverse transcriptase (DNA control) or on RNA from the *glcP1* mutant did not result in any product (Fig. 4D, lanes 8 and 9 respectively).

Transcription of glcP1 *is induced by glucose*

The promoter activities were analysed *in vivo* in a complementary experiment by taking advantage of the *redD* promoter probe system (van Wezel *et al*., 2000). For this purpose, 242 bp DNA fragments containing either the *glcP1* or the *glcP2* upstream region (nt positions –192/+49 relative to the start of the respective genes) were placed in front of the promoterless *redD* gene. The resulting constructs pIJ2587-glcP1p and pIJ2587-glcP2p were introduced in the non-pigmented indicator strain *S. coelicolor* A3(2) M512, and grown on R2YE plates for 6 days (*Supplementary material*, Fig. S1). Production of the red-pigmented undecylprodigiosin (Red) was strongly stimulated by the presence of pIJ2587-glcP1p in M512, while no stimulation of Red production was observed in M512(pIJ2587-glcP2p). Hence, the data suggest that only *glcP1* was transcribed.

High resolution transcript analysis was used to study transcription of *glcP1* and *glcP2* in more detail. Nuclease S1 mapping experiments using probe GP1 revealed a single nuclease-protected band of 134 nt, corresponding to the *glcP1* transcript, with the A residue at nt position –86 (relative to the start of the gene) as the most likely transcriptional start site (Fig. 5A). Appropriate consensus –10 (TAGTCT) and –35 (TTGACT) sequences were found at the expected positions (*Supplementary material*, Fig. S1). These sequences corresponded well to the consensus sequences recognized by the $\acute{o}^{70}$-type major sigma factor HrdB of *S. coelicolor* (Strohl, 1992). In the reverse experiment, where we used a similar probe (called GP2), now designed to hybridize to *glcP2* mRNA, we could only detect a very faint band on the gel after prolonged exposure on the phosphorimager plate, again showing the very low transcriptional activity of the *glcP2* promoter (data not shown).

The onset of *glcP1* transcription was followed for 4 h after mycelia of the exponential phase had been transferred from complex medium to mineral medium. The inducibility of *glcP1* by glucose is underlined by the observation that maximal transcript levels were observed within 15 min after transfer to glucose-containing mineral medium (NMMP without casamino acids), with transcript levels decreasing significantly in time points later than 1 h (Fig. 4D). In contrast to in glucose-exposed cultures, *glcP1* transcription was only slightly elevated in mannitol-exposed cultures, and for a much shorter time. These data thus demonstrate the immediate expression of *glcP1* in response to glucose.

Discussion

Glucose is widely used in *Streptomyces* research as a preferred nutrient to study carbon source-dependent phenomena. Its utilization triggers CCR and delays the onset of antibiotic production and development (Angell *et al*., 1994; Kwakman and Postma, 1994; Bibb, 1996; Chater, 1998; Gagnat *et al*., 1999). Generally, transport and CCR

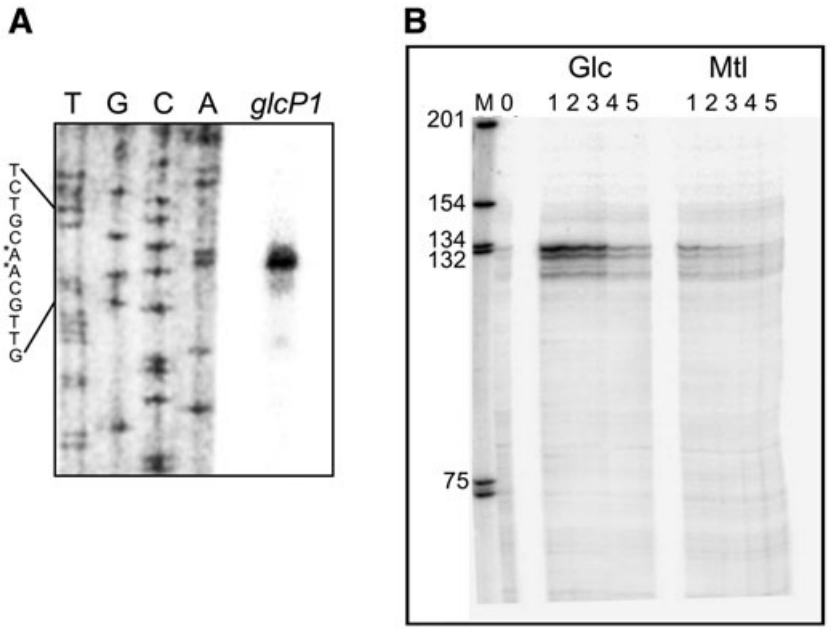

Fig. 5. Transcriptional analysis of *glcP*.
A. Mapping of the *glcP1* transcriptional start site. TGCA, DNA sequence ladder; *glcP1*, transcript derived from the *glcP1* promoter. The same sample was used as described in Fig. 5B (lane 1, Glc). The most likely transcriptional start sites are indicated by asterisks next to the DNA sequence.
B. Onset of *glcP1* transcription in *S. coelicolor* A3(2) M145. Mycelium from an exponentially growing liquid-grown TSB culture was harvested at OD_{550} = 0.6 and resuspended in NMMP with either glucose (Glc) or mannitol (Mtl) as the sole carbon source. RNA was isolated at various time points and analysed by nuclease S1 mapping. Lanes: M, molecular size marker (nt; ^{32}P-radiolabelled 1 kb ladder, Gibco BRL); 0, RNA isolated from TSB (t = 0 min); 1–5, samples corresponding to RNA isolated 15, 30, 60, 120 and 240 min after transfer from TSB to mineral medium respectively. The length of the full-sized transcript (approximately 134 nt) corresponds very well to the transcription start site predicted from the DNA sequence.

are closely linked, and to obtain more insight into the glucose-related phenomena, identification of the high-affinity transporter is a prerequisite (Brückner and Titgemeyer, 2002). Furthermore, several industrial streptomycetes, including the clavulanic acid producer *S. clavuligerus*, are not able to utilize glucose, and this most probably results from defective transport (Garcia-Dominguez *et al*., 1989). Thus, a better insight into the uptake of glucose by actinomycetes is important from both a fundamental and a biotechnological perspective. We here show that the glucose permease GlcP is a high-affinity glucose transporter that is indispensable to maintain the high growth rate on this carbon source, and thus constitutes the major glucose transporter. As a particular feature, we found that the gene for GlcP is duplicated, resulting in identical gene products.

Biochemical characterization of heterologously expressed GlcP suggests that the permease constitutes a H^+/symporter. A hydrophobicity analysis revealed a predicted topology of GlcP of six plus six transmembrane segments interrupted by a large cytoplasmic loop (*Supplementary material*, Fig. S2). These data are in accordance with the classification of GlcP as a member of the MFS, which includes either proton symporters or facilitator proteins of such a topology (Pao *et al*., 1998). Beside glucose, GlcP efficiently recognized 2-deoxyglucose, but not methyl α-glucoside, a feature also demonstrated for the homologous chicken liver glucose transporter Ch-GT2 (Wang *et al*., 1994). Fructose is not transported by GlcP, which distinguishes it from the bacterial glucose permeases from *Synechocystis* and *Z. mobilis* that represent the closest homologues (Zhang *et al*., 1989; Weisser *et al*., 1995). The functional expression of *glcP* in *E. coli* is to our knowledge the first demonstration of the production of a streptomycete membrane protein in this host.

In the bacterial world the transport of glucose is, with very few exceptions, mediated by glucose-specific PTSs that couple transport to phosphorylation (Postma *et al*., 1993). Previous studies indicated that *S. coelicolor* and other *Streptomyces* species do not have a glucose PTS (Titgemeyer *et al*., 1995; Parche *et al*., 2000). It was further assumed that *S. coelicolor* should have at least two transporters for glucose (see *Introduction*). Our data corroborate this assumption. We conclude that GlcP represents an efficient glucose uptake system. Elimination of GlcP leads to a significant reduction of the glucose growth rate and to loss of high-affinity uptake. As the GlcP-negative double mutant BAP19 was able to utilize glucose – although at a low rate – there should be at least one low-affinity system present. We failed to detect such a system in our transport assays, in which we measured so-called 'true uptake' that occurs in the range of seconds using sugar concentrations up to 1 mM. A constitutive low-affinity glucose transport activity (K_m of 6.1 mM) has been described earlier (Hodgson, 1982). The assay conditions used in this work and the late time points taken (10–60 min) were directed at monitoring slow uptake using millimolar glucose concentrations, and hence the high-affinity uptake system was not observed. Hurtubise *et al*. (1995) reported the presence of both a high- (K_m of 120 μM) and a low-affinity (K_m of 6.2 mM) glucose transport activity in *S. lividans*. The K_m of the high-affinity transport activity corresponded very well to what we have measured in *S. coelicolor* A3(2) mycelia (K_m of 137 μM).

These data are further consistent with our detection of a functional, almost identical *glcP* gene from *S. lividans* TK24 (Accession No. AF352022) that has four silent base substitutions compared with *S. coelicolor* A3(2) *glcP1*. However, the determined K_m of 41 μM for GlcP, when expressed in an *E. coli* mutant that is free of intrinsic glucose transport activity, was somewhat lower than the high-affinity K_m derived from *S. coelicolor* A3(2) mycelia. This difference might be explained by the possibility that the activity of GlcP differs slightly when expressed in the two different bacterial species. As for the low-affinity uptake, we propose that at least one permease perhaps with another sugar specificity may account for residual glucose incorporation. This is the case in *E. coli* that also uses the mannose- and galactose-specific permease for glucose import (Postma *et al*., 1993). Candidate genes have been recently described (Bertram *et al*., 2004). One of those could be encoded by the galactose permease gene *galP* that exhibits significant similarity to the glucose permease of *Vibrio parahaemolyticus* (Sarker *et al*., 1996).

The glucose transport experiment depicted in Fig. 4B showed an interesting feature that could not be explained easily from the GlcP activity alone. Expectedly, strains carrying a *glcP1* deletion showed only very weak transport. However, we did not anticipate that deletion of the almost silent *glcP2* should reproducibly result in a 40–50% reduction of overall GlcP transport activity, suggesting that *glcP1* is expressed at a lower level in the *glcP2* mutant. The existence of a second efficient transport system can be ruled out, as the *glcP1/glcP2* double mutant failed to transport glucose at an appreciable rate. This is further consistent with the observed reduced growth rates on glucose in strains lacking *glcP1*. Our RT-PCR data showed that indeed *glcP1* transcript levels were significantly reduced in the *glcP2* mutant. Intriguingly, we found that the most likely explanation for this apparent inconsistency was RNA interference, as we demonstrated that the apramycin resistance cassette inside *glcP2* generated high levels of an anti-sense transcript. This anti-sense transcript is complementary to *glcP1* transcripts over a stretch of 64 nt, allowing possible hybridization to the −36/+28 section of the sense transcript. Obviously, this will not only interfere with *glcP1* transcription, but certainly also with its efficient translation, as the ribosome binding site would be blocked for binding to the 3′ end of the 16S rRNA.

Transcriptional analysis revealed that the expression of *glcP1* was strongly inducible by glucose. Almost no expression of *glcP2* was detectable under the conditions tested, suggesting the latter is less important or plays a role under different culturing conditions. The first possibility is supported by the finding that *Streptomyces avermitilis* harbours only one *glcP* allele (SAV2657; annotated as a putative arabinose permease; 89% protein identity) (Ikeda *et al*., 2003). Inspection of the surrounding genes clearly shows that this is a homologue of *glcP1* of *S. coelicolor* A3(2). Moreover, *glcP2* is situated within the right variable arm of the *S. coelicolor* A3(2) genome, a region of genetic instability (Bentley *et al*., 2002). The possibility that *glcP2* is an active gene is supported by the facts that: (i) weak transcription of *glcP2* was observed, (ii) it encodes a functional product, and identical to GlcP1, suggesting evolutionary pressure or perhaps a very recent duplication event, and (iii) the *glcP1* and *glcP2* genes are preceded by the same 36 bp inverted repeat, which comprises the ribosome binding site and constitutes a possible binding site for a transcriptional regulator.

Beside the presence of *glcP* homologues in several *Streptomyces* species (89–100% protein identity), homologues are found in *Thermobifida fusca* [Accession No. ZP_00057880; 59% protein identity to GlcP of *S. coelicolor* A3(2)] and in other (non-sporulating) actinomycetes such as bifidobacteria, corynebacteria and mycobacteria. We have evidence that the *glcP* homologue of *Bifidobacterium longum* is a specific glucose permease (our unpublished results). For the others, experimental investigation remains to be awaited to answer the question whether glucose uptake via GlcP is widely spread among this class of bacteria.

In conclusion, the identification of GlcP as the main glucose transporter in *S. coelicolor* A3(2) sheds new light on the early stages of glucose-mediated processes in this important model organism. We are currently studying these relationships between glucose internalization via GlcP and glucose signalling concerning carbon regulation, antibiotic production and development.

Experimental procedures

Bacterial strains, plasmids, oligonucleotides and culture conditions

All strains and plasmids described in this article are presented in Table 1. The oligonucleotides used in this study are described in *Supplementary material* (Table S1). *E. coli* DH5α served as host for standard cloning procedures. The glucose transport-deficient *E. coli* strains LR2-175 and LM1 were used for heterologous complementation experiments (Lengeler *et al*., 1981; Aulkemeyer *et al*., 1991). *E. coli* ET12567(pUZ8002) was used for plasmid transfer via conjugation. *S. coelicolor* A3(2) strains M145 (SCP1$^-$ SCP2$^-$) and M512 (M145 Δ*redD* Δ*actII*-ORFIV), and *S. lividans* TK24 were obtained from the John Innes Centre strain collection. M512 was used as host for promoter probing experiments. pSU2718 (Martinez *et al*., 1988) and pBluescript II SK(+) were used for routine cloning experiments. pSET151, which contains a pUC origin of replication but is non-replicative in streptomycetes, was used for gene disruption experiments. *S. coelicolor* A3(2) and *S. lividans* strains were grown in tryptic soy broth without dextran (TSB; Difco) for isolation of

Table 1. Strains and plasmids used in this study.

Strains/plasmids	Genotype/description	Reference
Strains		
S. coelicolor A3(2)		
M145	SCP1$^-$, SCP2$^-$, prototroph	Hopwood *et al*. (1985)
M512	M145 Δ*redD* Δ*actII-ORF4*	Floriano and Bibb (1996)
BAP18	M145 Δ*glcP2::apr*	This work
BAP19	M145 Δ*lcP1::hyg*	This work
BAP20	M145 Δ*glcP1::apr* Δ*glcP2::hyg*	This work
S. lividans		
TK24	Wild type	Hopwood
E. coli		
DH5α	*supE44 lacU109 (ϕ80lacZ Δ M15M) hsdR17 recA1 endA1 gqrA96 thi-1 relA1*	Ausubel *et al*. (1990)
ET12567	F$^-$*dam*13::Tn9 *dcm6 hsdM hsd RrecF*143 *zjj*201::Tn10 *galK2 galT*22 *ara*-14 *lacY*1 *xyl-5 leuB*6 *thi*-1 *tonA*31 *rpsL*136 *hisG*4 *tsx*-78 *mtl*-1 *gln*V44	MacNeil *et al*. (1992)
LM1	*tonA, galT, nagE, manAI, kba$_{ts}$, rplI, xyl, metB, thi, his, mgla-C, argG, crr*	Lengeler *et al*. (1981)
LR2-175	*galP manA, nagE, glcA, fruA, mak*°	Aulkemeyer *et al*. (1991)
Plasmids		
pUZ8002	*oriT kan*, conjugation helper plasmid	Sia *et al*. (1996)
pBluescript II SK+	*bla*, high-copy cloning vector	Stratagene
pSU2718	*cat*, low-copy cloning vector	Martinez *et al*. (1988)
pFT76	pSU2718 with *glcP2 S. coelicolor* A3(2)	This work
pHPΩhyg	*hyg*, Hyg resistance cassette	M.-J. Virolle (unpubl.)
pHLW1	*aacC4*, Apr resistance cassette	Parche *et al*. (1999)
pSET151	*oriT* RK2 *bla tsr*	Hillemann *et al*. (1991)
pFT202	pBluescript II SK+ with *glcP1* downstream region	This work
pFT204	pSET151 with *glcP1* upstream region	This work
pFT205	pSET151 with *glcP2* upstream region	This work
pFT206	pBluescript II SK+ with *glcP2* downstream region	This work
pFT207	pFT204 with *glcP1* downstream region	This work
pFT209	pFT206 derivative, *apr*	This work
pFT211	pFT207 Δ*glcP1::hyg*	This work
pFT212	pFT205 Δ*glcP2::aacC4*	This work
pIJ2587	Promoter probe vector containing promoterless *redD* gene	van Wezel *et al*. (2000)
pIJ2587-glcP1p	pIJ2587 with *glcP1* promoter region (–192/+49 relative to the start of *glcP1*)	This work
pIJ2587-glcP2p	pIJ2587 with *glcP2* promoter region (–192/+49 relative to the start of *glcP2*)	This work

chromosomal DNA, and in mineral medium supplemented with 0.1–0.2% (w/v) casamino acids and 50 mM carbon source for growth curves and transport experiments (Kieser *et al*., 2000; Mahr *et al*., 2000; Nothaft *et al*., 2003b). *E. coli* strains were grown in Luria–Bertani (LB) broth at 37°C. The antibiotics ampicillin (100 mg l^{-1}), apramycin (25 mg l^{-1}), chloramphenicol (25 mg l^{-1}), hygromycin (100 mg l^{-1} for *S. coelicolor*; 200 mg l^{-1} for *E. coli*), kanamycin (60 mg l^{-1}) or thiostrepton (25 mg l^{-1}) were added where appropriate.

Cloning of glcP *genes*

Chromosomal DNA of *S. coelicolor* A3(2) M145 was isolated as described (Parche *et al*., 1999). A 1487 bp DNA fragment comprising the *glcP*-coding region of *S. coelicolor* A3(2) was amplified from chromosomal DNA by PCR with *Pfu* DNA polymerase using oligonucleotides GluT1 and GluT2. GluT1 was designed such as to provide stop codons in all three reading frames preceding the ribosomal binding site. The PCR fragment was digested with *Pst*I and cloned into pSU2718 digested with *Sma*I and *Pst*I in transcriptional fusion to the plasmid-borne *lacZ* promoter. The insertion was confirmed by DNA sequencing on an ABI PRISM 310 Genetic Analyzer (Perkin-Elmer) and the constructed plasmid was designated pFT76 (*glcP*$^+$).

Glucose transport assays

Transport assays for *S. coelicolor* A3(2) strains were performed as described previously (Nothaft *et al*., 2003b). *E. coli* strains were grown in LB supplemented with chloramphenicol (50 μg ml^{-1}) to an OD_{600} of 1.2–2.0. Cells were harvested by centrifugation, washed twice in transport buffer (50 mM Tris-HCl, pH 7.5, 50 mM NaCl, 10 mM KCl) and adjusted in the same buffer to an OD_{600} of 1.0. Cells were kept on ice and pre-incubated for 5 min at 37°C for the uptake assay. Uptake was initiated by addition of [U-C^{14}]-glucose at a final concentration of 20 or 100 μM (5 mCi mmol^{-1}). Samples (1 ml) were taken at different time points (10 s to 10 min) and treated as described (Nothaft *et al*., 2003b). The initial velocity of glucose incorporation was linear for at least 60 s. K_m and V_{max} were calculated from samples withdrawn after 10 s, using glucose concentrations ranging from 10 μM to 1 mM. Potential transport inhibitors (CCCP, 50 μM; DNP, 1 mM; DCCD, 0.5 mM; all purchased from Sigma) or non-radioactive sugars (10 mM) for the test of substrate specificity were added 1 min before addition of radio-labelled glucose (100 μM). Samples were collected after 1 min. It should be noted that the absolute transport activity of *S. coelicolor* A3(2) strains varied from experiment to experiment because of variation in the dispersity of the mycelia. We found that data between strains

were only comparable when grown in parallel in the same batch of medium.

Construction of glcP1/glcP2 *mutants*

The deletion vectors pFT211 for *glcP1* and pFT212 for *glcP2* were constructed as described below. Amplifications were performed with *S. coelicolor* A3(2) M145 chromosomal DNA. All PCR products were checked by DNA sequencing.

(i) Construction of pFT211 (Δ*glcP1*): a 924 bp fragment containing the *glcP1* downstream region was amplified with oligonucleotides GlcP1-1 and GlcP1-2. This PCR product was inserted as a *Bam*HI–*Eco*RI fragment into pBluescript II SK+, yielding pFT202. A 1007 bp fragment containing the *glcP1* upstream region was amplified with primers GlcP1-3 and GlcP1-4, and was cloned as a *Bam*HI–*Hin*dIII fragment into pSET151, giving pFT204. The *glcP1* downstream region was further cloned as a *Bam*HI–*Eco*RI fragment from pFT202 into pFT204, yielding pFT207. The hygromycin resistance cassette (*hyg*) was obtained from pHPΩhyg (M.-J. Virolle, unpubl.) and cloned as a *Bam*HI fragment in the same transcriptional orientation as *glcP1* into pFT207, yielding pFT211.

(ii) Construction of pFT212 (Δ*glcP2*): a 986 bp fragment containing the *glcP2* downstream region was amplified using oligonucleotides GlcP2-1 and GlcP2-2, and inserted as a *Bam*HI–*Eco*RI fragment into pBluescript II SK+ , yielding pFT206. A 988 bp fragment containing the *glcP2* upstream region was obtained by PCR with primers GlcP2-3 and GlcP2-4, and cloned as a *Hin*dIII–*Xba*I fragment into pSET151, giving plasmid pFT205. The apramycin resistance cassette (*aacC4*) was obtained from pHLW1 (Parche *et al*., 1999) and cloned in the same orientation as *glcP2* as a *Bam*HI–*Xba*I fragment into pFT206, yielding pFT209. The insert of pFT209 (*glcP2* downstream region preceded by *aacC4*) was then transferred as an *Xba*I–*Eco*RI fragment into pFT205, giving the final *glcP2* deletion vector pFT212.

Construction of the null mutants was achieved by conjugational transfer from ET12567(pUZ8002) harbouring pFT211 (Δ*glcP1::hyg*) or pFT212 (Δ*glcP2::aacC4*), respectively, to *S. coelicolor* A(3)2 M145 (Kieser *et al*., 2000). Ex-conjugants with the phenotype Hyg^r Tsr^s or Apr^r Tsr^s were clonally isolated. Sensitivity to thiostrepton (Tsr^s) was used as marker for loss of the non-replicating gene disruption vector, while resistance to hygromycin (Hyg^r) or apramycin (Apr^r) was a marker for the desired recombination event. The expected gene replacements were verified by PCRs that revealed the presence of the hygromycin and apramycin resistance cassettes (*hyg* and *aacC4*) and the correct chromosomal position, using oligonucleotides that hybridized in the antibiotic resistance gene and on the chromosome just outside the recombination area. One mutant ex-conjugant was designated BAP17 (Δ*glcP1::hyg*) and one BAP18 (Δ*glcP2::aacC4*). The same procedure was used to generate the double recombinant BAP20 (Δ*glcP1::hyg* Δ*glcP2::aacC4*) via conjugation of pFT212 into BAP17. The deleted regions comprised nt positions 34–1384 of *glcP1* and nt 29–1399 of *glcP2*.

RT-PCR analyses

RNA was prepared from cultures of *S. coelicolor* M145 grown for 40 h in 50 ml of mineral medium supplemented with 0.1% (w/v) casamino acids and with 50 mM glycerol or 50 mM glucose (Nothaft *et al*., 2003b). RT-PCR analyses were carried out with the one-step RT-PCR Kit (Qiagen) as described previously (Bertram *et al*., 2004). The quality of the RNA preparations was controlled by the presence of equal amounts of constitutively expressed 16S rRNA with oligonucleotides 16SRT-for and 16SRT-rev. RT-PCR experiments without prior reverse transcription were performed to assure exclusion of DNA contamination. For quantitative analysis, samples were taken at three-cycle intervals between cycles 18–35 to compare non-saturated PCR product formation. Data were verified in three independent experiments.

Streptomyces growth curves

Normal growth curves of *S. coelicolor* A3(2) M145 and its *glcP1*, *glcP2* and *glcP1glcP2* mutant derivatives were performed in 500 ml of NMMP cultures containing 50 mM glucose as the sole carbon source, and reduced concentration of casamino acids (0.2%). The strains were pre-grown for 16 h in NMMP + 50 mM mannitol; the mycelium was spun down, washed in NMMP without carbon source, and used to inoculate the main culture at a starting OD_{550} of 0.1. Cultures were grown at 30°C, under constant shaking (300 r.p.m.), and biomass accumulation was monitored by measuring the OD_{550}. In parallel, disappearance of glucose from the medium was monitored qualitatively using a glucose assay kit (Sigma).

Promoter probing experiments

For general assessment of promoter activity, we used the *redD* reporter system (van Wezel *et al*., 2000). The *redD* gene encodes the activator of the pathway for the red-pigmented tripyrrole undecylprodigiosine (Red). Promoter activity of DNA fragments cloned upstream of *redD* in the SCP2*-based plasmid pIJ2587 (around five copies per chromosome) results in accumulation of RedD and hence in rapid activation of Red biosynthesis in the indicator strain, *S. coelicolor* A3(2) M512; in the absence of promoter activity M512 is essentially unpigmented because of the absence of *redD* as well as *actII*-ORFIV, the activator for the *act* biosynthesis cluster. For assessing the activity of the *glcP1* and *glcP2* promoters, we analysed the −192/+49 regions (relative to the start of the respective genes). The *glcP1* promoter fragment was amplified by PCR using oligonucleotides GlcP11E and GlcP11B, and the *glcP2* promoter region was amplified using oligonucleotides GlcP21E and GlcP11B. In both cases, the oligonucleotides added an *Eco*RI and a *Bam*HI site to the upstream and downstream end of the fragments, respectively, allowing insertion of the fragment in the correct orientation in front of the promoterless *redD* gene. The constructs were named pIJ2587-glcP1p and pIJ2587-glcP2p for analysis of the *glcP1* and *glcP2* promoters respectively. Red production by the transformants on R2YE was monitored at approximately 12 h intervals during 6 days.

Nuclease S1 mapping

Total RNA was purified from liquid-grown NMMP cultures as

described (Kieser *et al*., 2000), except that DNase I treatment was used in addition to salt precipitation to fully eliminate DNA from the nucleic acid preparations. Appropriate primers (below) were labelled at their 5′ ends with [γ-^{32}P]-ATP with T4 polynucleotide kinase before DNA probes were produced by PCR. High-resolution S1 nuclease mapping was carried out as described previously (Kieser *et al*., 2000). For each RNA protection assay, excess of probe was hybridized to 30 μg of RNA. Protected fragments were analysed on denaturing 6% polyacrylamide gels, alongside a DNA sequencing ladder. Probes GP1 and GP2 were produced by PCR and used for mapping *glcP1* and *glcP2* transcripts respectively. Both correspond to the −192/+49 region. Probe GP1 was produced using oligonucleotides GlcP11E and GlcP-S1, and probe GP2 was produced using oligonucleotides GlcP21E and GlcP-S1. For the *glcP* induction experiments, mycelium from an exponentially growing TSB culture of *S. coelicolor* A3(2) M145 was harvested at an OD_{550} of 0.7 and resuspended in NMMP (but without casamino acids) with 50 mM glucose or 50 mM mannitol. RNA was isolated after 0, 15, 30, 60, 120 and 240 min and subjected to nuclease S1 mapping.

Computer analyses

The LaserGene workstation software (DNASTAR) was used to process DNA and protein sequence data. The *glcP* genes were identified by BLAST analysis of the *S. coelicolor* A3(2) genome (http://www.sanger.ac.uk/Projects/S_coelicolor). Protein databank searches were performed with the BLAST server of the National Center for Biotechnology Information at the National Institutes of Health Bethesda, MD, USA (http://www.ncbi.nlm.nih.gov). Hydrophobicity analysis was conducted using the TMPred algorithm (http://www.ch.embnet.org).

Acknowledgements

We thank Marie-Joëlle Virolle and Jan Kormanec for very fruitful discussions and Knut Jahreis for gift of *E. coli* strains. This work was funded by Grants SFB473, GK40 (to M.K. and K.M.), and GK805 (to E.F.P.S.) of the *Deutsche Forschungsgemeinschaft*, and by a grant from the Royal Netherlands Academy for Arts and Sciences (KNAW) to G.P.v.W.

Supplementary material

The following material is available from
http://www.blackwellpublishing.com/products/journals/suppmat/mmi/mmi4413/mmi4413.sm.htm

Fig. S1. *In vivo* promoter probe analysis of *glcP1* and *glcP2* and the sequence of the *glcP1* promoter region.
Fig. S2. Topology model of GlcP.
Table S1. List of oligonucleotides.

References

Angell, S., Lewis, C.G., Buttner, M.J., and Bibb, M.J. (1994) Glucose repression in *Streptomyces coelicolor* A3(2): a likely regulatory role for glucose kinase. *Mol Gen Genet* **244:** 135–143.

Aulkemeyer, P., Ebner, R., Heilenmann, G., Jahreis, K., Schmid, K., Wrieden, S., and Lengeler, J.W. (1991) Molecular analysis of two fructokinases involved in sucrose metabolism of enteric bacteria. *Mol Microbiol* **5:** 2913–2922.

Ausubel, F.A., Brent, R., Kingston, R.E., Moore, D.D., Seidmann, J.G., Smith, J.A., and Struhl, K. (1990) *Current Protocols in Molecular Biology*. New York: Greene Publishing and Wiley-Interscience.

Baltz, R.H. (1998) Genetic manipulation of antibiotic-producing *Streptomyces*. *Trends Microbiol* **6:** 76–83.

Bentley, S.D., Chater, K.F., Cerdeno-Tarraga, A.M., Challis, G.L., Thomson, N.R., James, K.D., *et al.* (2002) Complete genome sequence of the model actinomycete *Streptomyces coelicolor* A3(2). *Nature* **417:** 141–147.

Bertram, R., Schlicht, M., Mahr, K., Nothaft, H., Saier, M.H., Jr, and Titgemeyer, F. (2004) *In silico* and transcriptional analysis of carbohydrate uptake systems of *Streptomyces coelicolor* A3(2). *J Bacteriol* **186:** 1362–1373.

Bibb, M. (1996) 1995 Colworth Prize Lecture. The regulation of antibiotic production in *Streptomyces coelicolor* A3(2). *Microbiology* **142:** 1335–1344.

Brückner, R., and Titgemeyer, F. (2002) Carbon catabolite repression in bacteria: choice of the carbon source and autoregulatory limitation of sugar utilization. *FEMS Microbiol Lett* **209:** 141–148.

Chater, K.F. (1998) Taking a genetic scalpel to the *Streptomyces* colony. *Microbiology* **144:** 1465–1478.

Escalante, L., Ramos, I., Imriskova, I., Langley, E., and Sanchez, S. (1999) Glucose repression of anthracycline formation in *Streptomyces peucetius var. caesius*. *Appl Microbiol Biotechnol* **52:** 572–578.

Floriano, B., and Bibb, M. (1996) *afsR* is a pleiotropic but conditionally required regulatory gene for antibiotic production in *Streptomyces coelicolor* A3(2). *Mol Microbiol* **21:** 385–396.

Gagnat, J., Chouayekh, H., Gerbaud, C., Francou, F., and Virolle, M.J. (1999) Disruption of *sblA* in *Streptomyces lividans* permits expression of a heterologous alpha-amylase gene in the presence of glucose. *Microbiology* **145:** 2303–2312.

Garcia-Dominguez, M., Martin, J.F., and Liras, P. (1989) Characterization of sugar uptake in wild-type *Streptomyces clavuligerus*, which is impaired in glucose uptake, and in a glucose-utilizing mutant. *J Bacteriol* **171:** 6808–6814.

Hillemann, D., Pühler, A., and Wohlleben, W. (1991) Gene disruption and gene replacement in *Streptomyces* via single stranded DNA transformation of integration vectors. *Nucleic Acids Res* **19:** 727–731.

Hodgson, D.A. (1982) Glucose repression of carbon source uptake and metabolism in *Streptomyces coelicolor* A3(2) and its perturbation in mutants resistant to 2-deoxyglucose. *J Gen Microbiol* **128:** 2417–2430.

Hodgson, D.A. (2000) Primary metabolism and its control in streptomycetes: a most unusual group of bacteria. *Adv Microb Physiol* **42:** 47–238.

Hopwood, D.A., Bibb, M.J., Chater, K.F., Kieser, T., Bruton, C.J., Kieser, H.M., *et al.* (1985) *Genetic Manipulation of Streptomyces. A Laboratory Manual.* Norwich, UK: John Innes Foundation.

Hurtubise, Y., Shareck, F., Kluepfel, D., and Morosoli, R. (1995) A cellulase/xylanase-negative mutant of *Streptomyces lividans* 1326 defective in cellobiose and xylobiose uptake is mutated in a gene encoding a protein homologous to ATP-binding proteins. *Mol Microbiol* **17:** 367–377.

Ikeda, H., Ishikawa, J., Hanamoto, A., Shinose, M., Kikuchi, H., Shiba, T., *et al.* (2003) Complete genome sequence and comparative analysis of the industrial microorganism *Streptomyces avermitilis*. *Nat Biotechnol* **21:** 526–531.

Kieser, T., Bibb, M.J., Buttner, M.J., Chater, K.F., and Hopwood, D.A. (2000) *Practical Streptomyce Genetics.* Norwich, UK: The John Innes Foundation.

Kim, E.S., Hong, H.J., Choi, C.Y., and Cohen, S.N. (2001) Modulation of actinorhodin biosynthesis in *Streptomyces lividans* by glucose repression of *afsR2* gene transcription. *J Bacteriol* **183:** 2198–2203.

Kwakman, J.H., and Postma, P.W. (1994) Glucose kinase has a regulatory role in carbon catabolite repression in *Streptomyces coelicolor*. *J Bacteriol* **176:** 2694–2698.

Lengeler, J., Auburger, A.M., Mayer, R., and Pecher, A. (1981) The phosphoenolpyruvate-dependent carbohydrate: phosphotransferase system enzymes II as chemoreceptors in chemotaxis of *Escherichia coli* K 12. *Mol Gen Genet* **183:** 163–170.

MacNeil, D.J., Gewain, K.M., Ruby, C.L., Dezeny, G., Gibbons, P.H., and MacNeil, T. (1992) Analysis of *Streptomyces avermitilis* genes required for avermectin biosynthesis utilizing a novel integration vector. *Gene* **111:** 61–68.

Mahr, K., van Wezel, G.P., Svensson, C., Krengel, U., Bibb, M.J., and Titgemeyer, F. (2000) Glucose kinase of *Streptomyces coelicolor* A3(2): large-scale purification and biochemical analysis. *Antonie Van Leeuwenhoek* **78:** 253–261.

Martinez, E., Bartolome, B., and de la Cruz, F. (1988) pACYC184-derived cloning vectors containing the multiple cloning site and *lacZ* alpha reporter gene of pUC8/9 and pUC18/19 plasmids. *Gene* **68:** 159–162.

Nothaft, H., Dresel, D., Willimek, A., Mahr, K., Niederweis, M., and Titgemeyer, F. (2003a) The PTS of *Streptomyces coelicolor* is biased for *N*-acetylglucosamine metabolism. *J Bacteriol* **185:** 7019–7023.

Nothaft, H., Parche, S., Kamionka, A., and Titgemeyer, F. (2003b) *In vivo* analysis of HPr reveals a fructose-specific phosphotransferase system that confers high-affinity uptake in *Streptomyces coelicolor*. *J Bacteriol* **185:** 929–937.

Pao, S.S., Paulsen, I.T., and Saier, M.H., Jr (1998) Major facilitator superfamily. *Microbiol Mol Biol Rev* **62:** 1–34.

Parche, S., Schmid, R., and Titgemeyer, F. (1999) The phosphotransferase system (PTS) of *Streptomyces coelicolor*: identification and biochemical analysis of a histidine phosphocarrier protein HPr encoded by the gene *ptsH*. *Eur J Biochem* **265:** 308–317.

Parche, S., Nothaft, H., Kamionka, A., and Titgemeyer, F. (2000) Sugar uptake and utilisation in *Streptomyces coelicolor*: a PTS view to the genome. *Antonie Van Leeuwenhoek* **78:** 243–251.

Parker, C., Barnell, W.O., Snoep, J.L., Ingram, L.O., and Conway, T. (1995) Characterization of the *Zymomonas mobilis* glucose facilitator gene product (*glf*) in recombinant *Escherichia coli*: examination of transport mechanism, kinetics and the role of glucokinase in glucose transport. *Mol Microbiol* **15:** 795–802.

Pope, M.K., Green, B.D., and Westpheling, J. (1996) The *bld* mutants of *Streptomyces coelicolor* are defective in the regulation of carbon utilization, morphogenesis and cell–cell signalling. *Mol Microbiol* **19:** 747–756.

Postma, P.W., Lengeler, J.W., and Jacobson, G.R. (1993) Phosphoenolpyruvate: carbohydrate phosphotransferase systems of bacteria. *Microbiol Rev* **57:** 543–594.

Sabater, B., and Asensio, C. (1973) Transport of hexoses in *Streptomyces violaceoruber*. *Eur J Biochem* **39:** 201–205.

Sarker, R.I., Okabe, Y., Tsuda, M., and Tsuchiya, T. (1996) Sequence of a Na+/glucose symporter gene and its flanking regions of *Vibrio parahaemolyticus*. *Biochim Biophys Acta* **1281:** 1–4.

Schlösser, A. (2000) MsiK-dependent trehalose uptake in *Streptomyces reticuli*. *FEMS Microbiol Lett* **184:** 187–192.

Schlösser, A., and Schrempf, H. (1996) A lipid-anchored binding protein is a component of an ATP-dependent cellobiose/cellotriose-transport system from the cellulose degrader *Streptomyces reticuli*. *Eur J Biochem* **242:** 332–328.

Schlösser, A., Kampers, T., and Schrempf, H. (1997) The *Streptomyces* ATP-binding component MsiK assists in cellobiose and maltose transport. *J Bacteriol* **179:** 2092–2095.

Seo, J.W., Ohnishi, Y., Hirata, A., and Horinouchi, S. (2002) ATP-binding cassette transport system involved in regulation of morphological differentiation in response to glucose in *Streptomyces griseus*. *J Bacteriol* **184:** 91–103.

Sia, E.A., Kuehner, D.M., and Figurski, D.H. (1996) Mechanism of retrotransfer in conjugation: prior transfer of the conjugative plasmid is required. *J Bacteriol* **178:** 1457–1464.

Strohl, W.R. (1992) Compilation and analysis of DNA sequences associated with apparent streptomycete promoters. *Nucleic Acids Res* **20:** 961–974.

Titgemeyer, F., Walkenhorst, J., Reizer, J., Stuiver, M.H., Cui, X., and Saier, M.H., Jr (1995) Identification and characterization of phosphoenolpyruvate: fructose phosphotransferase systems in three *Streptomyces* species. *Microbiology* **141:** 51–58.

Ueda, K., Endo, K., Takano, H., Nishimoto, M., Kido, Y., Tomaru, Y., *et al.* (2000) Carbon-source-dependent transcriptional control involved in the initiation of cellular differentiation in *Streptomyces griseus*. *Antonie Van Leeuwenhoek* **78:** 263–268.

Wang, M.Y., Tsai, M.Y., and Wang, C. (1994) Identification of chicken liver glucose transporter. *Arch Biochem Biophys* **310:** 172–179.

Wang, F., Xiao, X., Saito, A., and Schrempf, H. (2002) *Streptomyces olivaceoviridis* possesses a phosphotransferase system that mediates specific, phosphoenolpyruvate-dependent uptake of *N*-acetylglucosamine. *Mol Genet Genomics* **268:** 344–351.

Weisser, P., Krämer, R., Sahm, H., and Sprenger, G.A. (1995) Functional expression of the glucose transporter of *Zymomonas mobilis* leads to restoration of glucose and fructose uptake in *Escherichia coli* mutants and provides evidence for its facilitator action. *J Bacteriol* **177:** 3351–3354.

van Wezel, G.P., White, J., Young, P., Postma, P.W., and Bibb, M.J. (1997) Substrate induction and glucose repression of maltose utilization by *Streptomyces coelicolor* A3(2) is controlled by *malR*, a member of the *lacI-galR* family of regulatory genes. *Mol Microbiol* **23:** 537–549.

van Wezel, G.P., White, J., Hoogvliet, G., and Bibb, M.J. (2000) Application of *redD*, the transcriptional activator gene of the undecylprodigiosin biosynthetic pathway, as a reporter for transcriptional activity in *Streptomyces coelicolor* A3(2) and *Streptomyces lividans*. *J Mol Microbiol Biotechnol* **2:** 551–556.

Zhang, C.C., Durand, M.C., Jeanjean, R., and Joset, F. (1989) Molecular and genetical analysis of the fructose-glucose transport system in the cyanobacterium *Synechocystis* PCC6803. *Mol Microbiol* **3:** 1221–1229.